

Phenomenological noise model for superconducting qubits: two-state fluctuators and $1/f$ noise

Dong Zhou and Robert Joynt

Department of Physics, University of Wisconsin-Madison, Wisconsin 53706, USA

(Dated: January 13, 2013)

We present a general phenomenological model for superconducting qubits subject to noise produced by two-state fluctuators whose couplings to the qubit are all roughly the same. In flux qubit experiments where the working point can be varied, it is possible to extract both the form of the noise spectrum and the number of fluctuators. We find that the noise has a broad spectrum consistent with $1/f$ noise and that the number of fluctuators with slow switching rates is surprisingly small: less than 100. If the fluctuators are interpreted as unpaired surface spins, then the size of their magnetic moments is surprisingly large.

PACS numbers: 03.65.Yz, 85.25.Cp, 85.25.Dq

I. INTRODUCTION

Superconducting qubits based on Josephson junctions are promising candidates for quantum information processing [1, 2]. Integrated-circuit fabrication technologies provides a relatively straightforward route to scale up the number of qubits, and the qubit coherence times have been prolonged dramatically since the superconducting charge, phase and flux qubit designs were first developed over a decade ago [3–6]. However, detailed mechanism of decoherence due to the coupling of the Josephson device to external noise sources is still not fully understood [1].

Recent experiments on superconducting qubits show that $1/f$ flux noise is an important source of decoherence [7–9]. Experiments over the years have agreed on certain universal characteristics of this noise: (1) it has weak dependence on a wide range of parameters such as SQUID loop geometry, inductance, material, etc.; (2) it has an approximately $1/f$ noise power spectrum and the magnitude ranges from $0.01 - 100(\mu\Phi_0)^2/Hz$ at the frequency $1Hz$, where $\Phi_0 = h/2e$ is the magnetic flux quantum [7–11].

The origin of this low-frequency noise at milli-Kelvin temperature has been a puzzle for over 20 years and is still under active debate [12–14]. There are indications that a high density of unpaired surface spins on the SQUIDs may be the physical causes of the noise [11, 12, 14–18]. These defect sites behave as two-state fluctuators that switches between their two states due to thermal activations and/or other interactions.

In this paper, we present a phenomenological model of the fluctuators. The physical parameters of the model can be extracted from qubit measurements at different working points. Analysis of experiments [7, 8] produces estimations of the effective magnetic moment and noise power spectrum density that are comparable to the experimental findings. Our chief new result is that the number of slow fluctuator is small, less than 100 and possible even of order 10.

The paper is organized as follows. In Sec. II, we describe and solve the model. This gives results for free

induction decay (FID), energy relaxation (ER) and spin echo (SE) signals. In Sec. III, we summarize our assumptions for the flux qubit systems and demonstrate how to extract the physical parameters of the model from experimental data. In Sec. IV we discuss the results.

II. NOISE MODEL

The superconducting flux qubits consist of a superconducting loop with three Josephson junctions [5]. The two relevant states are the clockwise and counter-clockwise persistent current states in the loop and the loop is effectively a quantum two-level system. The Hamiltonian of the superconducting flux qubit can be written as [1]

$$H_{qb} = -\frac{\varepsilon}{2}\sigma_z - \frac{\Delta}{2}\sigma_x - \frac{1}{2}h(t)\sigma_z, \quad (1)$$

where ε and Δ are the energy difference and tunneling splitting (Josephson coupling) between the clockwise and counter-clockwise current states, $h(t)$ is the flux noise in the environment and $\sigma_{x,y,z}$ are the Pauli matrices. The energy difference is proportional to the applied flux through the superconducting loop

$$\varepsilon = 2I_p(\Phi_{\text{ext}} - \Phi_0/2), \quad (2)$$

where I_p is the persistent current and Φ_{ext} is the externally applied magnetic flux in the loop. When Φ_{ext} is half a flux quantum, the two current states are degenerate in energy. The flux noise $h(t)$ is described by a time-dependent classical field. The eigenenergy of the qubit is thus

$$B_0 = \sqrt{\varepsilon^2 + \Delta^2}. \quad (3)$$

The angle $\theta = \tan^{-1}(\Delta/\varepsilon)$ is related to the working point of the device: $\theta = \pi/2$ is the optimal point and $\theta = 0$ is the pure dephasing point.

The flux noise is induced by an ensemble of fluctuators, all fluctuating independently, giving rise to random

telegraph noise (RTN). Assuming a total number of K fluctuators, the Hamiltonian can be written in the following form after a basis transformation

$$H = -\frac{1}{2}B_0\sigma_z - \frac{1}{2}\sum_{k=1}^K s_k(t)\vec{g}_k \cdot \vec{\sigma}. \quad (4)$$

Here we redefine the z -axis to be the eigenenergy axis. g_k is the coupling constant of the k 'th fluctuator. Note all fluctuators have the same θ value since flux fluctuation is along the ε direction. $s_k(t)$ is the random time sequence due to the k 'th fluctuator and switches between the two values -1 and 1 with an average switching rate γ_k . For a single fluctuator, the noise auto-correlation function is

$$\overline{s(t)s(t')} = \exp(-2\gamma|t - t'|). \quad (5)$$

the power spectrum is given by

$$\begin{aligned} S_{\text{RTN}}(\omega) &= \frac{g^2}{2\pi} \int_{-\infty}^{\infty} \overline{s(0)s(t)} e^{i\omega t} dt \\ &= \frac{1}{2\pi} \frac{4\gamma g^2}{\omega^2 + 4\gamma^2}. \end{aligned} \quad (6)$$

As is well-known, an ensemble of fluctuators with $1/\gamma$ distribution of their switching rates gives rise to $1/f$ noise power spectrum [19].

With the criteria

$$g_k \cos \theta \begin{cases} < \\ > \end{cases} \gamma_k \quad (7)$$

we can put the fluctuators into two categories, the fast ones ($<$) and slow ones ($>$). $K = M + N$ where M (N) is the number of slow (fast) fluctuators. The fast and slow fluctuators have qualitatively different effects on the qubit time evolution [20–24]. Fast is synonymous with weakly-coupled or Markovian, as can be seen from Eq. 7. The fast fluctuators can be treated with Redfield theory and they give rise to exponential decay of phase coherence. On the other hand, slow is synonymous to strongly-coupled or non-Markovian and Redfield theory cannot be applied. In general, for classical Markovian noise or Gaussian noise, the dephasing rates can be related to the noise spectral density and filter functions [25–27]. A list of filter functions for common pulsing sequences can be found in Table I of Ref. [27].

In this classical noise model, decoherence is a result of averaging the unitary time evolutions over all the possible noise sequences $s_k(t)$. The quasi-Hamiltonian method allows us to carry out this averaging analytically and treat the fast and slow fluctuators on an equal footing [20, 21]. The qubit dynamics is described by a transfer matrix acting on the qubit Bloch vector, i.e., $\vec{n}(t) = T(t)\vec{n}(t=0)$, while the transfer matrix is generated by a non-Hermitian quasi-Hamiltonian. In the case of a single qubit interacting with a single fluctuator, the

quasi-Hamiltonian has the form

$$H_q = -i\gamma + i\gamma\tau_1 + [B_0L_z + \tau_3 \otimes \vec{g} \cdot \vec{L}],$$

where τ_i are Pauli matrices associated with the fluctuator, and L_i are the $SO(3)$ generators associated with the qubit Bloch vector. Note the classical two-valued fluctuating field is mapped into a spin-1/2 particle in this formalism. The transfer matrix is given by $T(t) = \langle x_f | \exp(-iH_q t) | i_f \rangle$ where $|i_f\rangle = |x_f\rangle = [1; 1]/\sqrt{2}$ correspond to unbiased fluctuator. Exact diagonalization of H_q is possible only for $\theta = 0$ while perturbation expansion can be used in general to calculate the transfer matrix $T(t)$.

Signals from common experimental pulsing protocols, such as energy relaxation (ER), Hahn spin echo (SE) and free-induction (FID), can be calculated with the quasi-Hamiltonian method as well [21]. For these pulsing schemes, the qubit is initially in the ground state and the probability of the qubit being in the excited state is measured at time t . In the ER scheme, a single π pulse is applied at the beginning of the measurement. In the FID scheme, two $\pi/2$ pulses are applied, one at the beginning and the other at the end. The SE scheme has the two $\pi/2$ pulses as in the FID scheme and another π pulse in the middle of the time evolution, i.e., $t/2$. For our qubit-fluctuators model, the pulsed signals are given by

$$n_{\text{ER}}(t) \simeq e^{-(2\sum_m \gamma_m \epsilon_{2m}^2 \sin^2 \theta + \Gamma_1)t} \quad (8)$$

$$n_{\text{SE}}(t) \simeq e^{-(\Gamma_2 + \Gamma_3)t} \left[1 + \sum_{m=1}^M \epsilon_{1m} \sin(g_m \cos \theta t) \right] \quad (9)$$

$$\begin{aligned} n_{\text{FID}}(t) &\simeq e^{-(\Gamma_2 + \Gamma_3)t} \cos B_0 t \prod_{m=1}^M \cos(g_m \cos \theta t) \\ &\quad \left[1 + \sum_{m=1}^M \epsilon_{1m} \tan(g_m \cos \theta t) \right] \end{aligned} \quad (10)$$

where the relaxation and dephasing rates are given by

$$\Gamma_1 = \sum_{n=1}^N \frac{2\gamma_n g_n^2 \sin^2 \theta}{4\gamma_n^2 + B_0^2}, \quad (11)$$

$$\Gamma_2 = \frac{\Gamma_1}{2} + \Gamma_\phi \quad (12)$$

$$\Gamma_3 = \sum_{m=1}^M \gamma_m \quad (13)$$

$$\Gamma_\phi = \sum_{n=1}^N \frac{g_n^2 \cos^2 \theta}{2\gamma_n}. \quad (14)$$

Here $\epsilon_{1m} = \gamma_m / (g_m \cos \theta)$ and $\epsilon_{2m} = g_m / B_0$ are the small parameters of the perturbation theory.

The decoherence rates $\Gamma_1 = 1/T_1$, $\Gamma_2 = 1/T_2$ and Γ_ϕ are caused by the fast fluctuators and the equations for

them are consistent with Redfield results [25]. In the case of a single fast fluctuator, the decoherence rates for the echo experiment can be directly connected to the noise power spectral density, i.e., $1/T_1 = \sin^2 \theta S_{\text{RTN}}(B_0)$, $1/T_\phi = \cos^2 \theta S_{\text{RTN}}(0)$ and $1/T_2 = 1/2T_1 + 1/T_\phi$. Γ_3 is entirely due to the slow fluctuators.

III. DETERMINATION OF MODEL PARAMETERS FROM EXPERIMENTAL DATA

For purposes of data analysis, it is necessary for us to specify a not completely general but yet still flexible model for the noise. Let $d(\gamma) = \sum_{k=1}^K \delta(\gamma - \gamma_k)$ be the distribution of rates and take g to be independent of k , i.e., $g_k = g$. If there is a range of couplings then g in the following formulas can be regarded as an appropriate average coupling. This equal-coupling-strength or single-coupling-strength assumption should not be a severe limitation of our model as long as the standard deviation in the distribution of g_k 's is small relative to g itself, and to the width of the distribution of γ_k 's. For the specific case of fluctuating magnetic moments producing flux noise, the model is appropriate if the moments are all on the surface of the superconducting loop. We will comment further on this below.

We will assume a broad noise spectrum by taking

$$d(\gamma) = \begin{cases} \alpha \gamma^{s-1}, & \text{for } \gamma_{\min} < \gamma < \gamma_{\max} \\ 0, & \text{otherwise.} \end{cases} \quad (15)$$

Here γ_{\max} and γ_{\min} are the upper and lower cuts of the fluctuators' switching rates. For 1/f noise we must have $\gamma_{\min} > 0$ and $\gamma_{\max} < \infty$ in order that the energy density of the noise be finite. The power-law assumption is often useful for analyzing experimental data, though the method used to solve the model itself is capable of treating arbitrary distributions. Note $s = 0$ gives 1/f noise.

Under those assumptions, the pulsed signals are given by

$$n_{\text{ER}}(t) \simeq e^{-\Gamma_1 t} \quad (16)$$

$$n_{\text{SE}}(t) \simeq e^{-(\Gamma_2 + \Gamma_3)t} \left[1 + \frac{\Gamma_3}{\gamma_c} \sin(\gamma_c t) \right] \quad (17)$$

$$n_{\text{FID}}(t) \simeq e^{-(\Gamma_2 + \Gamma_3)t} \cos B_0 t \cos^M(\gamma_c t) \left[1 + \frac{\Gamma_3}{\gamma_c} \tan(\gamma_c t) \right] \quad (18)$$

where $\gamma_c = g \cos \theta$ is the critical coupling strength. The task of data analysis is then to determine the five intrinsic parameters g , α , s , γ_{\min} , and γ_{\max} from observations of the pulsed signals n_{ER} , n_{FID} and n_{SE} . The formulas show that the ER and SE signals at different working points alone are enough to fully determine all the five parameters, at least in principle. The FID data provide consistency checks and, crucially, to find the number of slow fluctuators at various working points. We have an-

alyzed data from Ref. [7, 8] and all results are listed in Table I.

For the ease of analysis, it is convenient to define

$$\Phi_{\text{SE}}(t, \theta) = \frac{n_{\text{SE}}(\theta)}{n_{\text{SE}}(\theta = \pi/2)} = e^{-\Gamma_3 t} \left[1 + \frac{\Gamma_3}{\gamma_c} \sin \gamma_c t \right], \quad (19)$$

where $\Phi_{\text{SE}}(t, \theta = 0)$ correspond to the 'phase-memory functional' defined by other authors [24, 28]. Note Γ_1 has only weak dependence on the working point θ , thus $\Gamma_2(\theta) \simeq \Gamma_1(\theta = \pi/2)/2$, and it drops out in Eq. 19.

Similarly, we define Φ_{FID} or the FID signal

$$\Phi_{\text{FID}}(t, \theta) = \frac{n_{\text{FID}}(\theta)}{n_{\text{FID}}(\theta = \pi/2)} = e^{-\Gamma_3 t} \left[1 + \frac{\Gamma_3}{\gamma_c} \tan \gamma_c t \right] \cos^M(\gamma_c t). \quad (20)$$

It is important to note that Φ_{FID} has explicit dependence on the number of slow RTN fluctuators M .

We note the scaling parameter s has significant effect on the working point dependence of the decoherence rates, especially for Γ_3 . In the case of 1/f noise, $s = 0$ and we have

$$\Gamma_1 \simeq \frac{\alpha g^2 \sin^2 \theta}{B_0} \tan^{-1} \left(\frac{2\gamma_{\max}}{B_0} \right) \quad (21)$$

$$\Gamma_2 \simeq \frac{\Gamma_1}{2} + \frac{\alpha}{2} \gamma_c \quad (22)$$

$$\Gamma_3 \simeq \alpha(\gamma_c - \gamma_{\min}). \quad (23)$$

Note Γ_3 has linear relationship to γ_c in this case.

If $s = 1$,

$$\Gamma_1 \simeq \frac{\alpha g^2 \sin^2 \theta}{4} \log \left(\frac{B_0^2 + 4\gamma_{\max}^2}{B_0^2 + 4\gamma_c^2} \right) \quad (24)$$

$$\Gamma_2 \simeq \frac{\Gamma_1}{2} + \frac{\alpha \gamma_c^2}{2} \log \frac{\gamma_{\max}}{\gamma_c} \quad (25)$$

$$\Gamma_3 \simeq \frac{\alpha}{2} (\gamma_c^2 - \gamma_{\min}^2). \quad (26)$$

In general,

$$\Gamma_1 \simeq \frac{2\alpha \sin^2 \theta g^2 \gamma^{s+1}}{B_0^2(s+1)} {}_2F_1 \left(1, \frac{s+1}{2}; \frac{s+1}{2} + 1; -\frac{4\gamma^2}{B_0^2} \right) \quad (27)$$

$$\Gamma_2 \simeq \frac{\Gamma_1}{2} + \frac{\alpha \gamma_c^2}{2(s-1)} (\gamma_{\max}^{s-1} - \gamma_c^{s-1}) \quad (28)$$

$$\Gamma_3 \simeq \frac{\alpha}{s+1} (\gamma_c^{s+1} - \gamma_{\min}^{s+1}). \quad (29)$$

Here ${}_2F_1$ is the hypergeometric function.

In flux qubit experiments, the working point is experimentally tunable by varying the applied flux and $\gamma_c = g \cos \theta$ changes accordingly. Thus a plot of Γ_3 ver-

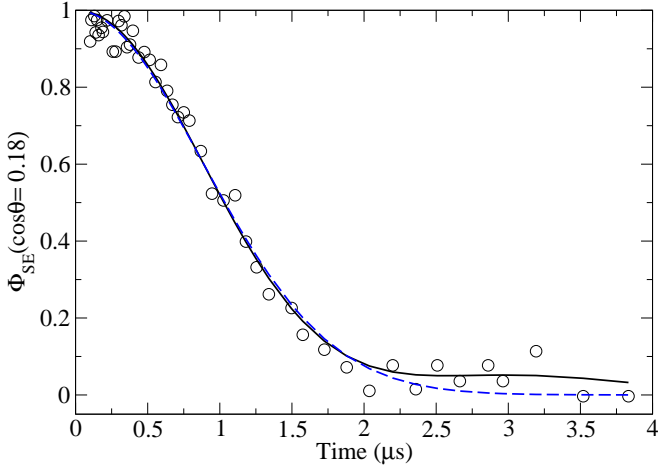


FIG. 1. (Color Online) Echo phase memory functional Φ_{SE} data in Fig.4A of Ref.[7]. We fit the 36 data points (open circle) to Eq.19 (black solid line) and Gaussian model $\Phi_{SE}^G = e^{-\Gamma_G^2 t^2}$ (blue dashed line) respectively.

sus γ_c would unambiguously determine the distribution of the fluctuators $d(\gamma)$.

A. coupling constant g

To extract the coupling constant g , we fit the phase memory functional to Eq. 19, as seen in Fig. 1. Thus for each working point θ , we can extract two numbers from the fitting, i.e. $\Gamma_3(\theta)$ and $\gamma_c(\theta)$. For example, the data in Fig. 1 were taken at working point $\cos\theta = 0.18$, and the corresponding $\Gamma_3 = 0.99$ MHz and $\gamma_c = 2.1$ MHz.

In Ref. [7, 8], the same data is fitted to a Gaussian noise model where the Gaussian flux fluctuation assumes a $1/f$ noise spectral density, i.e., $S_\phi(\omega) = A/\omega$. In this case, the phase memory functional takes the Gaussian form $\Phi_{SE}^G = e^{-\Gamma_G^2 t^2}$. As seen in Fig. 1, both models fit the data well and it is unclear which model is better. Non-Gaussian behavior manifests itself unambiguously with ‘plateaus’ in the phase memory functional Φ_{SE} [24, 28]. The rise in the longer time in Fig. 1 could be the onset of such ‘plateaus’. A cleaner sample with fewer surface spins (smaller α) would help to make the ‘plateaus’ more visible, which would then distinguish the present model from the Gaussian model [21].

With data at different working point θ , we can plot γ_c versus $\cos\theta$. The coupling constant g is the slope, as seen in Fig.2(a) ¹. Similar data analysis for Ref. [7] has been carried out in Ref. [21].

¹ In the data analysis, we first extract Γ_G from Ref. [7, 8], then reproduce Φ_{SE}^G from the Gaussian formula. Given Φ_{SE}^G fits the real experimental data well, we fit the reproduced Φ_{SE}^G to Eq. 19 to obtain Γ_3 and γ_c at different working points.

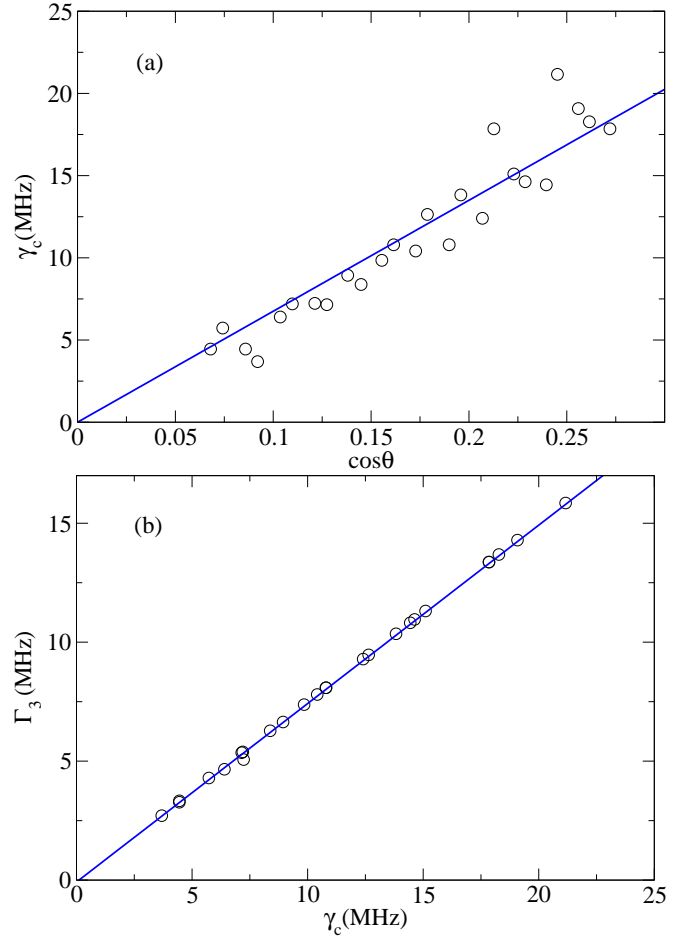


FIG. 2. Fitting of data from Ref.[8]. Both γ_c and Γ_3 are fitted from Φ_{SE} at various working point. (a) Critical rate γ_c versus the working point $\cos\theta$. The slope is the coupling constant g . (b) Linear regression to $\Gamma_3 = \alpha(\gamma_c - \gamma_{\min})$.

B. noise intensity α , noise index s and lower cut γ_{\min}

The functional form of Γ_3 allows us to determine α , s and γ_{\min} , as seen in Eq. 29.

Fitting the data from Ref. [8] we get clean linear dependence of γ_c , as seen in Fig. 2(b). A similar result has been obtained in Ref. [21] for the data from Ref. [7]. This is a sign of $1/f$ noise in the environment ($s = 0$). γ_{\min} is the intercept of the linear fit. Unfortunately, its accuracy depends strongly on the quality of the data at low γ_c , and the data are lacking in that region. Hence there is considerable uncertainty in the fitted value of γ_{\min} . The noise intensity α can be retrieved from the slope, in the case of $1/f$ noise, as seen in Eq. 23.

If s is taken as a fitting parameter as well, we get $s = -0.005$ for Ref. [8] and $s = -0.07$ for Ref. [7]. Thus the data is consistent with $1/f$ noise and we adopted the linear fit as in Eq. 23. When the noise power spectral density deviates farther from $1/f$, there are indications that as s decreases from 0, the pure dephasing time T_ϕ

	A	B
Δ/h (GHz)	5.445	3.9
ε/h (GHz)	0 ~ 1	0 ~ 1.1
I_p (nA)	160	370
r (μm)	1	2
$\Gamma_1^{(ex)}$ (MHz)	0.65	7.1
g/h (MHz)	9.5(0.2)	68(2)
γ_{\min} (MHz)	0.05(0.01)	0.11(0.05)
α	0.77(0.006)	0.754(0.003)
$\Gamma_1^{(th)}$ (MHz)	0.02(0.01)	1.4(0.1)
m (μ_B)	$1.7(0.03) \times 10^3$	$5.2(0.2) \times 10^3$
$S_\Phi(\omega = 1\text{Hz})$ (Φ_0^2/Hz)	$3.5(0.2) \times 10^{-11}$	$3.3(0.2) \times 10^{-10}$

TABLE I. Noise characteristics extracted from Ref.[7] (column A) and Ref.[8] (column B). The numbers in the top portion are experimental data while the ones in the lower portion are derived parameters from the model. The numbers in the parenthesis are standard deviations from linear regression.

also decreases [29].

C. upper cutoff γ_{\max}

For general s , Γ_1 can be expressed in terms of hypergeometric function in s . In the case of $1/f$ noise, $s = 0$ and we have Eq. 21. Since γ_{\max} is the only unknown in the equation (Γ_1 is experimentally measurable and the other quantities can be derived from the experiment), γ_{\max} can be extracted, at least in principle. But for the data in Ref. [7, 8], we are unable to back out γ_{\max} . One finds $\tan^{-1}(2\gamma_{\max}/B_0)$ has to be greater than $\pi/2$ to validate the equation.

The lack of experimental accuracy might not help for this self-inconsistency. One possible remedy is that there is some other source of high frequency noise, other than RTN, to cause relaxation. Thus the experimentally observed Γ_1 , as denoted by $\Gamma_1^{(ex)}$ in Table I is actually greater than $\Gamma_1^{(th)} = \pi\alpha g^2/2B_0$ which only includes the energy relaxation due to the fluctuators. Here $\Gamma_1^{(th)}$ is defined with $\gamma_{\max} = \infty$ and $\theta = \pi/2$ for Eq. 21.

D. number of fluctuators K

Since most of the parameters in the model can be derived from the experimental data for n_{SE} and n_{ER} , we may use the data for n_{FID} to get a value for $M(\theta)$, the number of slow fluctuators. As seen in Eq. 20, the FID signal has explicit dependence on M . It is easiest to analyze this using the logarithm of the phase memory functional $\mathcal{K}_E(t)$.

For the Echo signal, the logarithm of the phase memory functional $\mathcal{K}_E(t)$ can be expanded in terms of $\gamma_c t \ll 1$

and we have

$$\mathcal{K}_E(t) \equiv -\log \Phi_{SE} \simeq \begin{cases} \Gamma_3 \gamma_c^2 t^3 / 6, & \gamma_c t \gg \Gamma_3 / \gamma_c, \\ \Gamma_3^2 t^2 / 2, & \gamma_c t \ll \Gamma_3 / \gamma_c. \end{cases} \quad (30)$$

Similarly, we define \mathcal{K}_F for the envelope of FID signal. In the limit of $\gamma_c t \ll 1$,

$$\mathcal{K}_F(t) \equiv -\log \Phi_{FID}, \simeq \frac{M\gamma_c^2 + \Gamma_3^2}{2} t^2. \quad (31)$$

Note at small times ($\gamma_c t \ll \Gamma_3 / \gamma_c$), both $\mathcal{K}_E(t)$ and $\mathcal{K}_F(t)$ are quadratic in time. If the waiting time for the first plateau is too long comparing to the damping time $\tau_D \simeq 1/\Gamma_3$, both phase memory functionals will assume Gaussian shape. In the experiments [7, 8], the authors fit to the quadratic terms in Eqs. 30 and 31. What they called $\Gamma_{\phi E}^g$ and $\Gamma_{\phi F}^g$ correspond to $\Gamma_3/\sqrt{2}$, and $\sqrt{(M\gamma_c^2 + \Gamma_3^2)/2}$.

In Ref. [7], $\Gamma_{\phi F}^g \simeq 8\Gamma_{\phi E}^g$. This linear dependence is expected as long as the qubit is not operated extremely close to the optimal point $\theta = \pi/2$, as can be seen from Eq. 23. Thus the number of slow fluctuators $M \simeq 64\Gamma_3^2/\gamma_c^2$ is of the order 10 for the working points in the experiment. To be more specific,

$$M \sim 64 \times \alpha^2 \sim 38. \quad (32)$$

It should be evident that this is a rough estimate. However, it is unlikely to be off by order of magnitude and we assert that $M < 100$.

E. effective magnetic moment and power spectrum

As a consistency check, we find the magnetic moment associated with the fluctuators and the total spectral density. The change in flux due to spin in the SQUID loop is

$$\Delta\Phi = \frac{\mu_0}{r} m \quad (33)$$

where m is the effective magnetic moment of the spin, μ_0 is the magnetic constant and r is the radius of the loop.

For flux qubit, we have

$$\Delta\Phi = \frac{g}{2I_p}, \quad (34)$$

where I_p is persistent current along the qubit loop. Thus

$$m = \frac{rg}{2\mu_0 I_p}. \quad (35)$$

The noise power spectrum density is

$$\begin{aligned}
 S_{1/f}(\omega) &= \int_{\gamma_{\min}}^{\gamma_{\max}} S_{\text{RTN}}(\omega) d(\gamma) d\gamma \\
 &\simeq \frac{g^2}{\pi\omega} \left[\tan^{-1} \left(\frac{2\gamma_{\max}}{\omega} \right) - \tan^{-1} \left(\frac{2\gamma_{\min}}{\omega} \right) \right] \\
 &\simeq \frac{\alpha g^2}{2\omega}
 \end{aligned} \tag{36}$$

With Eq. 34, the noise power spectrum density in terms of flux is

$$S_{\Phi}(\omega) = S_{1/f}(\omega)/4I_p^2. \tag{37}$$

These derived results are listed in Table I.

IV. CONCLUSION

We have given a method for extracting the properties of the two-state fluctuators that cause decoherence in superconducting qubits. This method applies when the working point of the qubit can be varied, as is possible in flux qubit set-ups. The shape and strength of the noise spectrum can be determined from qubit measurements, and an estimate of the total number of active slow fluctuators can be obtained. We analyze two experiments

and find that the number of slow fluctuators is surprisingly small, less than 100. If we assume that the noise arises from magnetic clusters on the surface of the superconducting loop, then the size of the magnetic moment of the clusters is quite large, of the order of 1000 to 5000 μ_B .

These results appear to be rather surprising. However, a recent analysis [30] of noise measurements on dc SQUID inductance [18] suggests that the predominant noise sources are large magnetic clusters and that such clusters would give rise to 1/f-like noise. This gives rise to a consistent picture of two quite different qubits analyzed in two quite different ways.

The quasi-Hamiltonian method is applicable to more complex systems as well, such as interacting two-qubit systems [31]. An extension of the current work would be to examine the more recent experiment where the dephasing of two inductively coupled flux qubits are studied [16].

ACKNOWLEDGMENTS

We thank Robert McDermott, J. S. Tsai and K. Kechedzhi for helpful discussions and Zhigeng Geng for teaching the authors to use R (the programming language and software environment for statistical computing and graphics). This work is supported by the DARPA/MTO QuEST program through a grant from AFOSR.

-
- [1] J. Clarke and F. Wilhelm, *Nature* **453**, 1031 (2008)
 - [2] Y. Makhlin, G. Schön, and A. Shnirman, *Rev. Mod. Phys.* **73**, 357 (May 2001)
 - [3] Y. Nakamura, C. Chen, and J. Tsai, *Physical Review Letters* **79**, 2328 (Sep. 1997) V. Bouchiat, D. Vion, P. Joyez, D. Esteve, and M. H. Devoret, *Physica Scripta* **T76**, 165 (1998) Y. Nakamura, Y. Pashkin, and J. Tsai, *Nature* **398**, 786 (1999) D. Vion, a. Aassime, a. Cottet, P. Joyez, H. Pothier, C. Urbina, D. Esteve, and M. H. Devoret, *Science (New York, N.Y.)* **296**, 886 (May 2002)
 - [4] Y. Yu, S. Han, X. Chu, S.-I. Chu, and Z. Wang, *Science (New York, N.Y.)* **296**, 889 (May 2002) J. Martinis, S. Nam, J. Aumentado, and C. Urbina, *Physical Review Letters* **89**, 117901 (Aug. 2002) A. Berkley, H. Xu, R. Ramos, M. Gubrud, F. Strauch, P. Johnson, J. Anderson, A. Dragt, C. Lobb, and F. Wellstood, *Science* **300**, 1548 (2003)
 - [5] J. E. Mooij, T. P. Orlando, L. Levitov, L. Tian, van der Wal, C. H., and S. Lloyd, *Science* **285**, 1036 (Aug. 1999) C. H. van der Wal, A. C. J. ter Haar, F. K. Wilhelm, R. N. Schouten, C. J. P. M. Harmans, T. P. Orlando, S. Lloyd, and J. E. Mooij, *ibid.* **290**, 773 (Oct. 2000) J. Friedman, V. Patel, W. Chen, S. Tolpygo, and J. Lukens, *Nature* **406**, 43 (Jul. 2000) I. Chiorescu, Y. Nakamura, C. J. P. M. Harmans, and J. E. Mooij, *Science (New York, N.Y.)* **299**, 1869 (Mar. 2003)
 - [6] H. Paik, D. Schuster, L. Bishop, G. Kirchmair, G. Catelani, a. Sears, B. Johnson, M. Reagor, L. Frunzio, L. Glazman, S. Girvin, M. Devoret, and R. Schoelkopf, *Physical Review Letters* **107**, 1 (Dec. 2011)
 - [7] F. Yoshihara, K. Harrabi, A. O. Niskanen, Y. Nakamura, and J. S. Tsai, *Phys. Rev. Lett.* **97**, 167001 (Oct. 2006)
 - [8] K. Kakuyanagi, T. Meno, S. Saito, H. Nakano, K. Semba, H. Takayanagi, F. Deppe, and A. Shnirman, *Phys. Rev. Lett.* **98**, 47004 (Jan. 2007)
 - [9] F. C. Wellstood, C. Urbina, and J. Clarke, *Appl. Phys. Lett.* **50**, 772 (1987)
 - [10] V. Foglietti, W. J. Gallagher, M. B. Ketchen, A. W. Kleinsasser, R. H. Koch, S. I. Raider, and R. L. Sandstrom, *Appl. Phys. Lett.* **49**, 1393 (1986)
 - [11] R. C. Bialczak, R. McDermott, M. Ansmann, M. Hofheinz, N. Katz, E. Lucero, M. Neeley, A. D. O'Connell, H. Wang, A. N. Cleland, and J. M. Martinis, *Phys. Rev. Lett.* **99**, 187006 (Nov. 2007)
 - [12] R. H. Koch, D. P. DiVincenzo, and J. Clarke, *Phys. Rev. Lett.* **98**, 267003 (Jun. 2007)
 - [13] L. Faoro and L. B. Ioffe, *Phys. Rev. Lett.* **100**, 227005 (Jun. 2008)
 - [14] R. de Sousa, *Phys. Rev. B* **76**, 245306 (Dec. 2007)
 - [15] S. Sendelbach, D. Hover, A. Kittel, M. Mück, J. M. Martinis, and R. McDermott, *Phys. Rev. Lett.* **100**, 227006 (Jun. 2008)
 - [16] F. Yoshihara, Y. Nakamura, and J. S. Tsai, *Physical Review B* **81**, 132502 (Apr. 2010)
 - [17] S. Gustavsson, J. Bylander, F. Yan, W. Oliver, F. Yoshihara, and Y. Nakamura, *Physical Review B* **84**, 014525 (Jul. 2011)

- [18] S. Sendelbach, D. Hover, M. Mück, and R. McDermott, Phys. Rev. Lett. **103**, 117001 (Sep. 2009)
- [19] S. Kogan, *Electronic Noise and Fluctuations in Solids* (Cambridge University Press, 2008)
- [20] R. Joynt, D. Zhou, and Q.-H. Wang, Int. J. Mod. B **25**, 2115 (2011)
- [21] D. Zhou and R. Joynt, Phys. Rev. A **81**, 10103 (Jan. 2010)
- [22] D. Zhou, A. Lang, and R. Joynt, Quant. Info. Processing **9**, 727 (Mar. 2010)
- [23] E. Paladino, L. Faoro, G. Falci, and R. Fazio, Phys. Rev. Lett. **88**, 228304 (May 2002)
- [24] Y. M. Galperin, B. L. Altshuler, J. Bergli, and D. V. Shantsev, Phys. Rev. Lett. **96**, 97009 (Mar. 2006)
- [25] C. P. Slichter, *Principles of Magnetic Resonance*, third edit ed. (Springer, New York, 1996)
- [26] J. M. Martinis, S. Nam, J. Aumentado, K. M. Lang, and C. Urbina, Phys. Rev. B **67**, 94510 (Mar. 2003)
- [27] L. Cywinski, R. M. Lutchyn, C. P. Nave, and S. Das Sarma, Phys. Rev. B **77**, 174509 (May 2008)
- [28] Y. M. Galperin, B. L. Altshuler, J. Bergli, D. Shantsev, and V. Vinokur, Phys. Rev. B **76**, 64531 (Aug. 2007)
- [29] S. Anton, C. Mueller, J. Birenbaum, S. O'Kelley, A. Fefferman, D. Golubev, G. Hilton, H. Cho, K. Irwin, F. Wellstood, G. Schoen, A. Shnirman, and J. Clarke, Arxiv preprint arXiv:1111.7272, 1(2011) arXiv:arXiv:1111.7272v1,
- [30] K. Kechedzhi, L. Faoro, and L. B. Ioffe(2011) arXiv:1102.3445 [cond-mat]
- [31] A. De, A. Lang, D. Zhou, and R. Joynt, Physical Review A **83**, 42331 (Apr. 2011)